ACS APPLIED MATERIALS & INTERFACES

Research Article

www.acsami.org

Polythiolactone-Based Redox-Responsive Layers for the Reversible Release of Functional Molecules

Sabrina Belbekhouche,[†] Stefan Reinicke,[‡] Pieter Espeel,[‡] Filip E. Du Prez,[‡] Pierre Eloy,[†] Christine Dupont-Gillain,[†] Alain M. Jonas,[†] Sophie Demoustier-Champagne,*[,†] and Karine Glinel*[,†]

[†]Institute of Condensed Matter & Nanosciences (Bio & Soft Matter), Université catholique de Louvain, Croix du Sud 1, box L7.04.01, B-1348 Louvain-La-Neuve, Belgium

[‡]Polymer Chemistry Research Group, Department of Organic and Macromolecular Chemistry, Ghent University, Krijgslaan 281 S4, B-9000 Ghent, Belgium

Supporting Information

ABSTRACT: The development of thin macromolecular layers with incorporated disulfide bonds that can be disrupted and formed again under redox stimulation is of general interest for drug release applications, because such layers can provide rapid and reversible responses to specific biological systems and signals. However, the preparation of such layers from polythiols remains difficult, because of the fast oxidation of thiol groups in ambient conditions. Here we propose water-soluble thiolactone-containing copolymers as stable precursors containing protected thiol groups, allowing us to produce on demand polythiol layers on gold substrates in the presence of amine derivatives. Electrochemical, water contact angle, X-ray photoelectron spectroscopy, and X-ray reflectometry measurements evidence the formation of uniform copolymer layers containing both anchored and free thiol groups. The number of free thiols increases with the content of thiolactone units in the copolymers. In a second step, a thiolated dye, used as a model drug, was successfully grafted on the free thiol groups through disulfide bonds using mild oxidizing conditions, as proved by fluorescence and quartz crystal microbalance measurements. Finally, the reversible release/regrafting of the dye under redox stimulation is demonstrated.

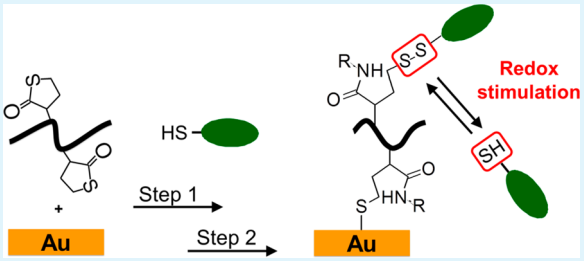

KEYWORDS: *disulfide link, polythiol, thiolactone aminolysis, stimuli-responsive polymer, gold surface modification, responsive surface, drug release*

INTRODUCTION

Controlling the release of drugs from surfaces is a critical issue for developing efficient and optimized advanced drug delivery systems.[1−3] In the past decade, dedicated research enabled the development of various stimuli-responsive polymer-based drug delivery coatings that are capable of releasing therapeutic agents based on the application of specific stimuli.[4,5] These systems present a significant advantage over conventional therapies, being the ability to regulate spatially and temporally the drug release profile for optimal therapeutic efficacy.[6,7] Several mechanisms are exploited to trigger cargo release from stimuli-responsive polymer layers, including changes in pH and temperature, enzymatic degradation and redox-activated cleavage.[4−15] Among them, redox-responsive systems based on the reversible formation/scission of disulfide bonds have emerged as a very promising class of biomedical materials for the development of sophisticated delivery systems as they offer a rapid response under stimulation.[10−15] Moreover, they can be stimulated by the cells themselves.[10−19] Indeed, disulfide bonds are extremely stable in physiological conditions but can react with the exofacial thiols located on the cell membrane.[19] In addition, when penetrating the cell membrane, they are rapidly cleaved in the strongly reducing environment of the cytoplasm.[20,21] Altogether, these features can be advantageously used to direct the delivery of drugs into cells.[22]

A possible approach to prepare such layers consists of the immobilization on material surfaces of derivatives bearing free thiol groups such as polythiols.[23] These layers can be subsequently grafted with a thiol-derived drug through a disulfide bond.[24] However, polythiols are prone to oxidation which considerably limits their manipulation.[25] Therefore, we opted for the implementation of thiolactone-based chemistry for the versatile and straightforward preparation of decorated gold surfaces.[26] As introduced by Espeel et al. in 2011,[27] thiolactone chemistry is a valuable synthetic tool, in addition to established thiol-X conjugation reactions, and has been used for polymer synthesis[28,29] and postpolymerization modification,[30−33] hydrogel formation,[34] and solid-supported, sequence-controlled chain elongation.[35]

Received: September 21, 2014
Accepted: November 26, 2014
Published: December 1, 2014

Scheme 1. Synthesis of P(DMA-*co*-TlaAm)-*x* Copolymers by RAFT Polymerization

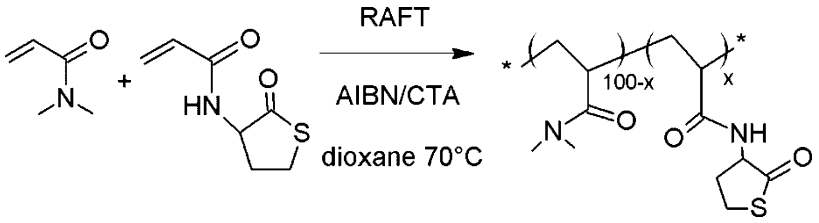

Scheme 2. Methodology Developed to Prepare Redox Responsive Copolymer Layers onto Gold Surfaces

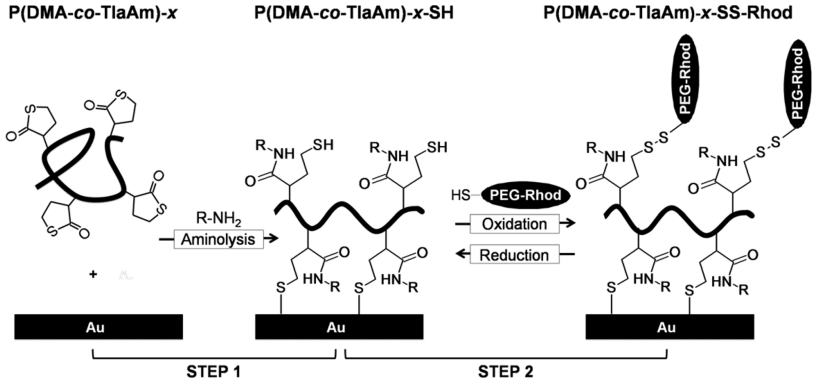

Herein, we show that statistical copolymers containing thiolactone units can be efficiently used as stable precursors of polythiols, in a one-pot gold surface-modification protocol. Copolymers of the readily available thiolactone acrylamide (TlaAm) and *N*,*N*-dimethylacrylamide (DMA), containing various contents of thiolactone, were synthesized by Reversible Addition−Fragmentation chain Transfer (RAFT) polymerization. These polythiolactones, releasing free thiol groups in the presence of amine derivatives, were then successfully grafted onto flat gold surfaces. The most appealing feature of this grafting approach is the simultaneous modification of the polymer backbone by incorporation of various amine residues and the immobilization of the generated polythiols onto gold substrates, allowing for the versatile preparation of diversely substituted surfaces. The characteristics of the different coatings were systematically measured by X-ray photoelectron spectroscopy (XPS), cyclic voltammetry and contact angle measurements. In a second step, a thiol-functionalized fluorescent dye, used as a model drug, was installed on the free thiol groups of the copolymer layers via a redox cleavable disulfide link. Finally, the release of the dye under redox stimulation was investigated by fluorescence microscopy, quartz crystal microbalance and electrochemical impedance spectroscopy.

EXPERIMENTAL SECTION

Materials. 2,2′-Azobis(isobutyronitrile) (AIBN) (Sigma-Aldrich) was recrystallized twice from methanol. *N*,*N*-Dimethylacrylamide (DMA) (Sigma-Aldrich, 99%) was passed over a column filled with activated, basic alumina (Sigma-Aldrich, Brockmann I) before usage. The thiolactone acrylamide (TlaAm) monomer and the chain transfer agent (CTA) 2-{[(butylsulfanyl)-carbonothioyl]sulfanyl}propanoic acid were synthesized according to protocols described in ref 31. The following chemicals were used as received: ethanolamine (Sigma-Aldrich, 99+ %), 4-fluorobenzylamine (Sigma-Aldrich, 97%), *N*-chloro-*p*-toluenesulfonamide sodium salt trihydrate (CaT) (Sigma-Aldrich, 98%), *threo*-1,4-dimercapto-2,3-butanediol (DTT) (Sigma-Aldrich, 99+ %), potassium hexacyanoferrate (III) (Sigma-Aldrich, 99+ %), potassium hexacyanoferrate (II) trihydrate (Sigma-Aldrich, 99.5+ %), potassium chloride (KCl) (Sigma-Aldrich), 4-(2-hydroxyethyl)-1-piperazineethanesulfonic acid (HEPES) (Sigma-Aldrich, 99.5+ %), 2-(*N*-morpholino)ethanesulfonic acid (MES) (Sigma-Aldrich, 99.5+ %), chloroform ($CHCl_3$) (Sigma-Aldrich, 99.5+ %, anhydrous), *N*,*N*-dimethylformamide (DMF) (Sigma-Aldrich, 99.8%, anhydrous), 1,4-dioxane (Sigma-Aldrich, 99.8%, anhydrous), diethyl ether (Sigma-Aldrich, 99+ %, anhydrous), ethanol (VWR, HPLC grade), hydrogen peroxide (Sigma-Aldrich, 30%), sulfuric acid (Sigma-Aldrich), rhodamine B-poly(ethylene glycol)-thiol (Rhod B-PEG-SH) (Interchim, M_W = 3 400 g mol^{-1}). Gold nanoparticles with a diameter of 40 nm and stabilized in citrate buffer (2×10^{11} particles.mL^{-1}) were kindly supplied by Coris Bioconcept company. Water was purified with a Milli-Q reagent system (Millipore).

Gold-coated surfaces were fabricated in a clean room (Winfab platform, UCL) environment by evaporating a 100 nm thick layer of gold on 1 × 1 cm^2 silicon wafers (100) precoated with a 10 nm thick layer of titanium.

Synthesis of P(DMA-*co*-TlaAm) Copolymers. Statistical copolymers based on DMA and TlaAm were synthesized by RAFT polymerization according to a recent procedure.[31] Scheme 1 shows the involved reaction. Typically, for the preparation of a copolymer containing 30% TlaAm, 3.05 g (30.8 mmol) of DMA, 2.53 g (13.2 mmol) of TlaAm, 2.9 mg (0.018 mmol) of AIBN, and 41.8 mg (0.18 mmol) of CTA were dissolved in 20 mL of dioxane ($[M]_0/[CTA]/[AIBN]$ = 250/1/0.1). The solution was transferred into a Schlenk tube and degassed by 4−5 freeze−pump−thaw cycles. After that, the tube was immersed in a thermostated oil bath set to 70 °C and the solution was stirred for 4 h. The polymerization was stopped by immersing the Schlenk tube in an ice/water bath followed by exposure of the polymerization solution to air. The final polymer was obtained by repeated precipitation into diethyl ether. Different P(DMA-*co*-TLaAm) copolymers containing various contents of TlaAm were synthesized by varying the initial DMA: TlaAm monomer ratio. These copolymers will be named P(DMA-*co*-TlaAm)-*x* in the sequel, with *x* denoting the theoretical percentage of TlaAm units incorporated in the copolymer.

Aminolysis of P(DMA-*co*-TlaAm) Copolymers. The ring-opening of thiolactone groups of P(DMA-*co*-TlaAm) upon amine treatment was tested in solution. For example, 10 mg of P(DMA-*co*-TlaAm)-30 (i.e., 30 μmol of TlaAm unit) were dissolved in 5 mL of chloroform, and 60 μmol of amine (i.e., 2 mol equiv compared to TlaAm units), dissolved in 36.6 μL of chloroform, were added. This

solution was placed in a small glass flask and left to react for 2 h. The polymer was then precipitated in 20 mL of diethyl ether, rinsed with 5 mL of diethyl ether and dried at 70 °C for 12 h. The aminolyzed copolymers will be named P(DMA-*co*-TlaAm)-*x*-SH in the sequel, with *x* denoting the theoretical percentage of TlaAm units incorporated initially in the copolymer.

Immobilization of P(DMA-*co*-TlaAm) Copolymers onto Flat Gold Surfaces. All glassware was cleaned using piranha solution, a 50:50 v/v mixture of hydrogen peroxide (30%) and sulfuric acid (***Caution:*** *piranha solution is extremely reactive and should be handled carefully*). One × one cm^2 gold surfaces were first cleaned with water and ethanol, then treated in a UV/ozone chamber (UVO-Cleaner, Jelight) for 20 min. After an additional rinsing with ethanol, surfaces were dried under N_2 flow. This whole process was repeated twice. The grafting of P(DMA-*co*-TlaAm) copolymers onto gold surfaces was performed in the presence of ethanolamine or 4-fluorobenzylamine according to the reaction described in Scheme 2 (step 1). Typically, 10 mg of copolymer (i.e., 30 μmol of TlaAm unit) was dissolved in 5 mL of chloroform in a small glass flask, and 60 μmol of amine (i.e., 2 mol equiv compared to TlaAm units) dissolved in 36.6 μL of chloroform were added. This solution was quickly stirred (~10 s) and a freshly cleaned gold surface was immediately added in the flask. After a contact time of 2 h, the surface was thoroughly rinsed with chloroform, ethanol, and Milli-Q water and then dried with a stream of N_2.

Immobilization of P(DMA-*co*-TlaAm)-30 Copolymer on Gold Nanoparticles. One hundred microliters of a suspension of gold nanoparticles (2×10^{11}particles.mL^{-1}), 2.8 mg (i.e., 8.4 μmol of TlaAm unit) of P(DMA-*co*-TlaAm)-30, 16.4 μmol of ethanolamine (i.e., 2 mol equiv compared to TlaAm units) and 1.4 mL of DMF were mixed in a 2.5 mL Eppendorf tube. The suspension was gently stirred with a micro magnetic bar for 2 h, then centrifuged at 11 700 *g* for 10 min and the supernatant was removed. Approximately 1.4 mL of DMF was added in the tube and the nanoparticles were redispersed by agitation with a vortex. This rinsing process was repeated three times.

Grafting of Rhod B-PEG-SH on a P(DMA-*co*-TlaAm)-30 Layer. Fluorescent Rhod B-PEG-SH derivative was immobilized onto the free thiol groups of a P(DMA-*co*-TlaAm) layer through the formation of a disulfide bond (Scheme 2, step 2). A 1 × 1 cm^2 gold surface modified with a P(DMA-*co*-TlaAm)-30 layer was placed in a 2 cm diameter glass dish. One mg (0.29 μmol) of Rhod-PEG-SH was dissolved in 1 mL of MES buffer (10 mM, pH 6) and 50 μL of this solution was deposited onto the gold surface. Then 2 mL of a 2 mM CaT solution in MES buffer (10 mM, pH 6) was added. After a contact time of 1 min, the surface was thoroughly rinsed with ethanol and then Milli-Q water. A similar procedure was used to graft Rhod B-PEG-SH onto gold nanoparticles coated with a P(DMA-*co*-TlaAm)-30 layer. Briefly,10 μL of a 0.3 mM Rhod B-PEG-SH solution in MES (10 mM, pH 6) and 100 μL of a suspension (2×10^{11} particles.mL^{-1}) of gold nanoparticles modified by P(DMA-*co*-TlaAm)-30 were mixed in a 2.5 mL Eppendorf tube. Then 1.4 mL of a 2 mM CaT solution in MES buffer (10 mM pH 6) was added and the tube was shaken for 1 min. The gold nanoparticles were subsequently rinsed three times with 1.4 mL MES buffer. The fluorescence measurements performed in the last supernatant testified for the absence of Rhod B-PEG-SH molecule. The copolymer layers grafted with Rhod B-PEG-SH will be named P(DMA-*co*-TlaAm)-*x*-SS-Rhod in the sequel.

Release of Grafted Rhod B-PEG-SH under Redox Stimulation. The release of Rhod B-PEG-SH grafted onto a P(DMA-*co*-TlaAm)-30 layer was tested in the presence of DTT, a reducing agent. A 1 × 1 cm^2 gold surface modified with P(DMA-*co*-TlaAm)-30-SS-Rhod was placed in a small flask and 2 mL of a 0.1 M DTT solution (in 10 mM HEPES buffer, pH 7.2) were added. After a contact time of 10 min, the surface was thoroughly rinsed with HEPES buffer (10 mM, pH 7.2). The release of labeled PEG derivative was evaluated by performing fluorescence microscopy and QCM-D measurements on the surface. A similar protocol was used to investigate the release of Rhod B-PEG-SH grafted on a P(DMA-*co*-TlaAm)-30 layer deposited on gold nanoparticles. One hundred microliters of a suspension (2×10^{11} particles.mL^{-1}) of modified gold nanoparticles was placed in 2.5 mL-Eppendorf tube and 1.4 mL of a 0.1 M DTT solution (in 10 mM HEPES buffer, pH 7.2) was added. The tube was shaken for 10 min, then centrifuged at 11 700 g for 10 min. The fluorescence of the supernatant was measured to quantify the amount of labeled PEG derivative released from the nanoparticles.

Characterization Techniques. *Elemental Analysis.* The chemical composition of P(DMA-*co*-TlaAm) copolymers was determined by elemental analysis performed on a Thermo Flash 2000 Automatic Elemental Analyzer. The percentages of carbon, nitrogen, hydrogen and sulfur were estimated and the content of thiolactone unit incorporated in copolymers was determined from the sulfur content.

Size Exclusion Chromatography (SEC). The average molar masses of P(DMA-*co*-TlaAm) copolymers were measured with a Waters instrument equipped with a Waters 2414 Refractive Index Detector and three PSS serial columns (GRAM Analytical 30 and 45, 1000 Å, 10 μm particle size) at 35 °C. Poly(methyl methacrylate) standards were used for calibration and LiBr-containing DMA (0.42 g L^{-1}) was used as an eluent at a flow rate of 1 mL min^{-1}. Average molar masses and dispersities ($Đ$) were determined using the Empower software.

Water Contact Angle Measurements. Static water contact angle measurements were carried out at room temperature with an OCA-20 apparatus (DataPhysics Instruments GmbH, Germany) in the sessile drop configuration. A drop (5 μL) of Milli-Q water was deposited onto the surface and the recorded image was analyzed by the SCA 20 software to determine the contact angle. At least three measurements were performed at different locations on the surface.

Electrochemical Measurements. Electrochemical characterizations were performed with a CHInstrument potentiostat 660B. All electrochemical experiments, including cyclic voltammetry (CV) and electrochemical impedance spectroscopy (EIS) were carried out at room temperature in a one-compartment Teflon cell with a platinum counter electrode, an Ag/AgCl reference electrode and copolymer-modified gold surfaces as working electrode. The barrier properties of the grafted layers were evaluated by studying the electron transfer reaction on the modified surfaces using a potassium ferrocyanide redox probe. The electrolytic solution contained equal concentrations of both the oxidized and reduced forms of the redox couple namely, 1 mM potassium ferrocyanide ($K_3Fe(CN)_6$), 1 mM potassium ferricyanide ($K_4Fe(CN)_6$) and 0.1 M KCl. All electrolyte solutions were purged with argon for at least 20 min prior to measurements. CV measurements were carried out by sweeping the potential between −0.3 and 0.6 V at a scan rate of 0.1 V s^{-1}. The blocking factor (BF), which is a good evaluation of the quality of the grafted layers, was calculated from the ratio between the difference of oxidation area of bare (A_{bare}) and modified (A_{mod}) gold substrates on CVs, and the oxidation area of modified gold substrate:

$$\mathrm{BF}(\%) = \left(\frac{A_{\mathrm{bare}} - A_{\mathrm{mod}}}{A_{\mathrm{bare}}}\right)100 \quad (1)$$

EIS measurements were made at the open circuit potential with a sinusoidal voltage perturbation amplitude of 10 mV in the frequency range of 1×10^{-1} to 1×10^{5} Hz.

The Nyquist plots were fitted by a Randles equivalent circuit derivative in order to estimate the charge transfer resistance (R_{ct}). This circuit consists of an element corresponding to the bulk solution resistance in series with a parallel combination of a constant phase element and Faradaic impedance (i.e., the charge transfer resistance and Warburg impedance representing respectively the interfacial electron transfer resistance and the diffusion of the redox probes in solution).[36]

The variation of the charge transfer resistance can be correlated with the gold surface coverage using eq 2[37]

$$\text{surface coverage} = 1 - \frac{R_{ct}^{0}}{R_{ct}} \quad (2)$$

Where R_{ct}^{0} and R_{ct} correspond to the charge transfer resistance measured on bare and modified gold surface, respectively.

Table 1. Characteristics of P(DMA-*co*-TlaAm)-*x* Copolymers Synthesized by RAFT Polymerization

copolymer	theoretical content in TlaAm units (%)[a]	experimental content in TlaAm units (%) determined by elemental analysis (%)	experimental content in TlaAm units (%) determined by XPS[b]	apparent average molar mass $\overline{M}_{ap}$ (g mol^{-1})[c]	dispersity Đ[c]
P(DMA-*co*-TlaAm)-5	5	6.3	5.9 ± 0.6	18 500	1.3
P(DMA-*co*-TlaAm)-10	10	10.6	12.4 ± 2.5	19 800	1.3
P(DMA-*co*-TlaAm)-15	15	14.3	16.1 ± 2.1	18 100	1.3
P(DMA-*co*-TlaAm)-30	30	34.5	36.3 ± 3.3	16 000	1.6

[a]Predicted from the initial monomer ratio. [b]Estimated from N/S and O/S ratio extracted from XPS measurements performed on dry copolymer powders. [c]Measured by SEC, in PMMA equivalents.

X-ray Photoelectron Spectroscopy (XPS). The analyses were performed on a Kratos Axis Ultra spectrometer (Kratos Analytical, Manchester, UK) equipped with a monochromatized Al X-ray source (powered at 10 mA and 15 kV). The modified gold samples were fixed on a standard stainless steel multispecimen holder by using a piece of double-sided insulating tape. The polymer powders were deposited on a piece of double-sided insulating tape, itself glued to a polyacetal plate fixed on the holder. The pressure in the analysis chamber was about 1 × 10^{-6} Pa. The direction of photoelectrons collection was perpendicular to the sample surface. Analyses were performed in the hybrid lens mode with the slot aperture, and the resulting analyzed area was 700 × 300 μm^2. The pass energy was set at 160 eV for the survey scan and 40 eV for narrow scans. In the latter conditions, the full width at half-maximum (fwhm) of the Ag $3d_{5/2}$ peak of a standard silver sample was about 0.9 eV. Charge stabilization was achieved by using the Kratos Axis device. The following sequence of spectra was recorded: survey spectrum, C 1s, O 1s, N 1s, S 2p, Si 2p (on powders only, to check for the absence of signal from the tape), Au 4f (on modified gold samples only), F 1s (whenever a fluorine-containing amine was used) and C 1s again to check for charge stability as a function of time and for absence of degradation of the sample during the analyses. The C-(C,H) component of the C 1s peak was fixed to 284.8 eV to set the binding energy scale. Molar fractions (%) were calculated using peak areas measured after linear background subtraction, and normalized on the basis of acquisition parameters, experimental sensitivity factors and transmission factors provided by the manufacturer. Data treatment was performed with the CasaXPS program (Casa Software Ltd., UK).The S 2p spectra were decomposed using a Gaussian/Lorentzian (70/30) product function, with the fwhm of the peak components kept identical.

The grafted copolymer layer attenuates the Au 4f XPS signal from the gold substrate. The thickness of the layer was estimated based on the $I_{C\ 1s}/I_{Au\ 4f}$ intensity ratio,[38,39] using eq 3, treating the copolymer as uniform with smooth boundaries

$$\frac{I_{Au}}{I_C} = \frac{\sigma_{Au}\lambda_{Au}^{Au}C_{Au}^{Au}\exp\left(-\frac{L}{\lambda_{Au}^{pol}}\right)}{\sigma_C\lambda_C^{pol}C_C^{pol}\exp\left(1-\frac{L}{\lambda_C^{pol}}\right)} \quad (3)$$

where L is the thickness of the grafted layer. I_{Au} and I_C represent C 1s and Au 4f peak intensities, respectively. λ is the inelastic mean free path in the considered medium, where pol stands for the copolymer (λ_{Au}^{gold} = 1.7 nm, λ_{Au}^{pol} = 4 nm and λ_C^{pol} = 3.5 nm).[40,41] σ is the photoemission cross section (σ_{Au} = 17.12 and σ_C = 1). C is the concentration of studied element in the considered medium (C_{Au}^{gold} = 0.1 mol cm^{-3}; λ_C^{pol} = 0.06 mol cm^{-3}). The effect of emission anisotropy was neglected.

Quartz Crystal Microbalance with Dissipation Monitoring (QCM-D). A Q-Sense E4(Q-Sense, Sweden) system employing AT-cut gold-coated quartz crystal sensors (Lot-Oriel, France) with a nominal frequency of about 5 MHz was used to monitor in situ the release of Rhod B-PEG-SH from P(DMA-*co*-TlaAm)-30 layer. The immobilization of the P(DMA-*co*-TlaAm)-30-SS-Rhod layer onto a sensor was performed as described above for flat gold surfaces. After mounting in the QCM-D flow chamber, the modified sensor was conditioned in HEPES buffer (10 mM HEPES pH 7.2) for 10 min. Then a 0.1 M DTT solution (in 10 mM HEPES pH 7.2) was injected into the cell with a flow rate of 50 μL.min^{-1} for 10 min. A rinsing of the chamber with HEPES buffer was subsequently performed for at least 90 min. During this process, the frequency shift (Δf) and the dissipation shift (ΔD) were recorded for all overtones. However, only the shifts acquired for the third overtone were considered for the data analysis. The measurements were performed at 25 °C. The mass variation (Δm) at the sensor surface was computed from Δf using Sauerbrey equation (eq 4) and assuming a rigid polymer layer[42]

$$\Delta m = -C_f\frac{\Delta f}{n} \quad (4)$$

with C_f being the sensitivity factor of the crystal sensor used (i.e., 17.7 ng cm^{-2} Hz^{-1}) and n the overtone number.

X-ray Reflectometry (XRR). The measurements were carried out with a modified Siemens D5000 2-circle goniometer (0.002° positioning accuracy). X-rays of 0.15418 nm wavelength (Cu Kα) were obtained from a Rigaku rotating anode operated at 40 kV and 300 mA, fitted with a collimating mirror (Osmic, Japan) delivering a close-to-parallel beam of ~0.0085° vertical angular divergence. The data were corrected for spillover and normalized to unit incident intensity, corrected for refraction effects in the gold, then scaled by the Fresnel reflectivity of bare gold and Fourier-transformed to obtain the autocorrelation function of the electron density gradient profile, as described fully elsewhere.[43] In order to amplify the sensitivity of the technique to the electron-poor organic layer, two measurements were performed successively, first for the film deposited over a thick gold layer of ca. 102 nm thickness resting over ca. 9.5 nm of Ti evaporated over a Si wafer; then for the very same sample over which a supplementary layer of gold of ca. 23 nm thickness was evaporated. The comparison between the autocorrelation functions before and after addition of the supplementary gold layer clearly revealed peaks associated with the correlation between the upper interface of the bottom gold layer and the lower and upper interfaces of the added external gold layer, from which the distance between the two gold layers, hence the organic film thickness, could be estimated (see the Supporting Information, Figure S1).

Epifluorescence Microscopy. The flat gold surfaces grafted with the fluorescent Rhod B-PEG-SH were observed with an optical inverted epifluorescence IX71 microscope (Olympus, Japan) equipped with a CCD camera and a fluorescence illuminator and various mirror units. Images were recorded at 40× magnification and processed using the Cell Sens Dimension 1.7 software (Olympus, Japan).

Fluorescence Spectroscopy. Fluorescence measurements were performed to quantify the amount of Rhod B-PEG-SH released from the surface of modified gold nanoparticles in the presence of DTT. For this, a 108-QS quartz cuvette (Hellma, Belgium) with an optical path length of 10 mm and a total volume of 1 mL was filled with 0.5 mL of supernatant obtained after DTT treatment then mounted in a Varian Carry Eclipse Fluorescence spectrophotometer (Agilent Technologies, Belgium). The measurements were performed with the excitation wavelength set at 544 nm and the emission spectrum recorded between 550 and 600 nm. A 0.1 M DTT solution in HEPES buffer was used as a blank. The amount of labeled PEG released in the supernatant was estimated from the intensity of the emission peak

occurring at 576 nm and a calibration curve established with standard solutions of Rhod B-PEG-SH.

Each surface characterization was performed at least in triplicate on three different freshly prepared samples.

RESULTS AND DISCUSSION

Synthesis of Thiolactone-Containing Copolymers. Water-soluble statistical copolymers, subsequently used as polythiol precursors, were synthesized by RAFT copolymerization of DMA and TlaAm monomers (Scheme 1). Four different copolymers were prepared, with a theoretical thiolactone content varying from 5 to 30% as predicted from the initial monomer ratio. Their experimentally determined thiolactone content, apparent average molar mass and dispersity are reported in Table 1. The obtained copolymers present similar molar masses of about 15−20 0×10^3 g mol^{-1}, with dispersities ranging from 1.3 to1.6. The content of TlaAm units effectively incorporated in the copolymers, determined by two independent methods (elemental analysis and XPS on copolymer powders) is in good agreement with the theoretical value.

Aminolysis of Copolymers. In our strategy, the formation of a linear polythiol from a thiolactone-based copolymer is performed by aminolysis (Scheme 2). In order to evaluate the efficiency of this reaction, it was first conducted in the absence of a gold surface. Since fluorine atoms are excellent markers for XPS analysis, aminolysis was tested by treating P(DMA-*co*-TlaAm)-30 with 4-fluorobenzylamine in chloroform solution. The XPS analysis performed on the resulting purified and dried polymer revealed a S/F ratio close to 1, which testified for the complete opening of the thiolactone rings in the presence of amines and consequently for the presence of thiol groups along the polymer chain.

Immobilization of Copolymers onto Flat Gold Surfaces. Next, the ability of P(DMA-*co*-TlaAm)-*x* copolymers to form linear polythiols by aminolysis was exploited to form in situ polythiol layers onto gold surfaces in one step (Scheme 2, step 1).

XPS measurements performed on such a layer obtained from P(DMA-*co*-TlaAm)-30 in the presence of 4-fluorobenzylamine showed Au, C, N, O, S, and F atoms on the surface (results not shown), in agreement with the immobilization of the copolymer onto the gold surface. Moreover, the S/F ratio was about 1, similar to what was obtained previously when P(DMA-*co*-TlaAm)-30 is treated in solution in the absence of a gold surface. This confirmed that the presence of the gold surface in the medium does not affect the aminolysis of the copolymer.

Considering that this study aims at preparing biofunctional layers, the aminolysis of the copolymers is pursued in the sequel by the hydrophilic ethanolamine derivative. To confirm the presence of the copolymer layer, static contact angle measurements were performed on flat gold surfaces before and after treatment by the copolymer and the amine. The contact angle decreased from ∼70° to ∼35° upon treatment, in agreement with the hydrophilic nature of introduced ethanolamine-residues. This variation in the surface wettability after copolymer grafting was found to be independent of the composition of P(DMA-*co*-TlaAm) (see the Supporting Information, Table S1).

The presence of the copolymer layer on the gold surface was also evidenced by performing CV measurements. In Figure 1, the bare gold surface shows a reversible voltammogram for the redox couple $[Fe(CN)_6]^{3-}/[Fe(CN)_6]^{4-}$ indicating that the electron transfer reaction is completely diffusion-controlled. In contrast, the absence of peak in the CVs of gold surfaces modified with aminolyzed P(DMA-*co*-TlaAm) copolymers evidences that the redox reaction is strongly inhibited due to the barrier resulting from the film deposition.[44] Interestingly, the profile of the voltammograms did not vary with the composition of the copolymer, indicating that the surface coverage was quite similar for all tested copolymers. The blocking factor, which is a good estimation for the quality of the grafted layers, was ca. 85−90% from eq 1. Longer reaction times between the copolymer solution and the gold surface did not further increase this blocking factor.

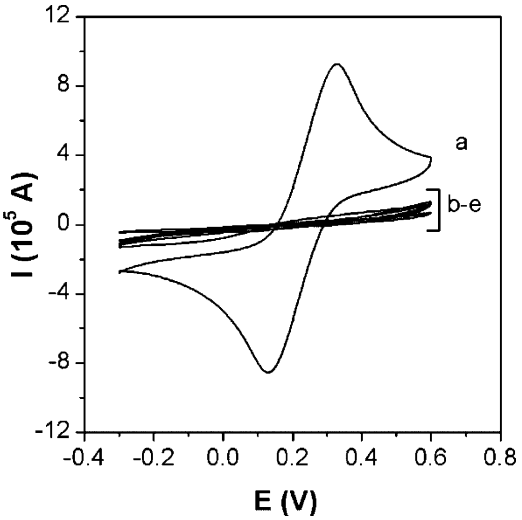

Figure 1. Cyclic voltammograms obtained on flat gold surfaces modified with copolymers aminolyzed with ethanolamine; the measurements were performed in the presence of $Fe(CN)_6^{3-/4-}$ (1 mM) solubilized in 0.1 M KCl at a scan rate of 0.1 $V.s^{-1}$: bare gold surface (a); gold surfaces modified with P(DMA-*co*-TlaAm)-*x*-SH with *x* = (b) 5, (c) 10, (d) 15, and (e) 30%.

XPS analysis also revealed a significant increase of the C/Au ratio from 0.35 for bare gold to ca. 0.8 or 1.0, for surfaces modified with P(DMA-*co*-TlaAm)-5,10,15-SH or P(DMA-*co*-TlaAm)-30-SH, respectively (see the Supporting Information, Table S1). This attenuation of the Au signal after copolymer treatment again demonstrates the presence of an organic layer on the surface.

The thickness of P(DMA-*co*-TlaAm)-15,30-SH copolymer layers immobilized onto gold surfaces was estimated by both XPS and XRR, using methodologies described in the Experimental Section. The results displayed in Table 2 show that both techniques are in agreement, providing values in the 2−4 nm range, which indicates that P(DMA-*co*-TlaAm)

Table 2. Thickness of the Copolymer Layers from XPS and XRR Measurements

	P(DMA-*co*-TlaAm)-*x*-SH		P(DMA-*co*-TlaAm)-*x*-SS-Rhod	
theoretical content (*x*) in TlaAm units in the copolymer (%)	XPS thickness[a] (nm)	XRR thickness[b] (nm)	XPS thickness[a] (nm)	XRR thickness[b] (nm)
15	1.5			
30	1.8	4	2.0	4

[a]Determined from eq 3. [b]Determined from the density profile of an Au substrate/copolymer layer/Au layer sample.

copolymers form very thin layers. The slight difference observed between both techniques can be attributed to the different sample preparation used for XPS and XRR, to differences in the measurement environment (ultrahigh vacuum for XPS, versus ambient for XRR), as well as to the errors and assumptions inherent to data modeling.

Quantification of Free Thiol Groups in Copolymer Layers. The thiol groups present on the aminolyzed copolymers offer the double benefit of anchoring the copolymer onto the gold surface and of in situ modification of the polymer chains by various thiol-X reactions or oxidative couplings (Scheme 2, step 2).[25,45] However, to achieve this subsequent functionalization on substrates grafted with aminolyzed copolymer chains, the presence of free residual thiol groups that are not anchored on the surface is required. XPS analyses were performed on the modified surfaces to estimate the content of free thiol groups. The XPS spectra measured with high energy resolution in the S 2p region are displayed in Figure 2 for grafted layers of copolymers with increasing thiolactone content (from A to D). The measured signal can be decomposed in two peaks centered on ~161.5 and ~163.5 eV, corresponding to sulfur atoms anchored (S_{Au}) or not (S_{SH}) to the gold surface, respectively.[46,47] Moreover, each peak is a doublet that can be decomposed in two components, corresponding to S $2p_{1/2}$ and S $2p_{3/2}$. For all tested copolymers, the intensity of the S_{Au} is higher than the one of S_{SH}. However, a significant increase of S_{SH} was observed with the increase of the TlaAm fraction in the copolymer. The relative amount of unbound sulfur atoms compared to anchored ones, computed from the total area of S $2p_{1/2}$ and S $2p_{3/2}$ peak corresponding to both groups, increased from 20 to 40% when the content in TlaAm units increased from 5 to 30% (Table 3). These results confirm the attachment of the aminolyzed copolymer chains onto the gold surface through a S–Au link. However, a significant amount of thiol groups present in the layer are still available and can be advantageously used for further functionalization of the layers. It is also important to note that some unbound thiol groups may have undergone oxidation during the surface treatment. This side reaction results in the formation of disulfide links between two thiol groups. Unfortunately the amount of disulfide groups in the layer could not be estimated since the XPS signal of sulfur atoms involved in thiol and disulfide groups cannot be discriminated.[48,49]

Stability of Copolymer Layers in Oxidizing Conditions. As mentioned above, free thiol groups in the copolymer layers can be used to graft functional molecules on the surface. A possible approach is to perform an oxidative coupling with a reagent bearing a thiol group, leading to the formation of a disulfide link (Scheme 2, step 2). Such a link is cleavable under redox stimulation and is therefore of interest for release applications. However, this methodology requires the stability of the copolymer layers in oxidizing medium. Chloramine T (CaT) was selected in this study for the oxidative coupling on the copolymer layers. Indeed, contrary to other oxidizing agents such as hydrogen peroxide[16] or hypochlorites,[50] CaT was shown to be a mild oxidant avoiding overoxidation reactions.[16,51,52] The stability of the copolymer layers immersed in a 2 mM CaT solution for different times was studied by CV. The variation of the BF values (eq 1) computed from the voltammograms, recorded before and after treatment, is displayed in Figure 3. The stability of the layers strongly increases with their content in TlaAm units. Indeed the BF measured after a treatment of 2500 min decreased to ca. 71 and 0% for P(DMA-*co*-TlaAm)-30-SH and P(DMA-*co*-TlaAm)-5-SH, respectively. Therefore, the larger the content in TlaAm in the copolymer, the higher the number of anchoring links between copolymer chains and surface, and the higher the layer stability.

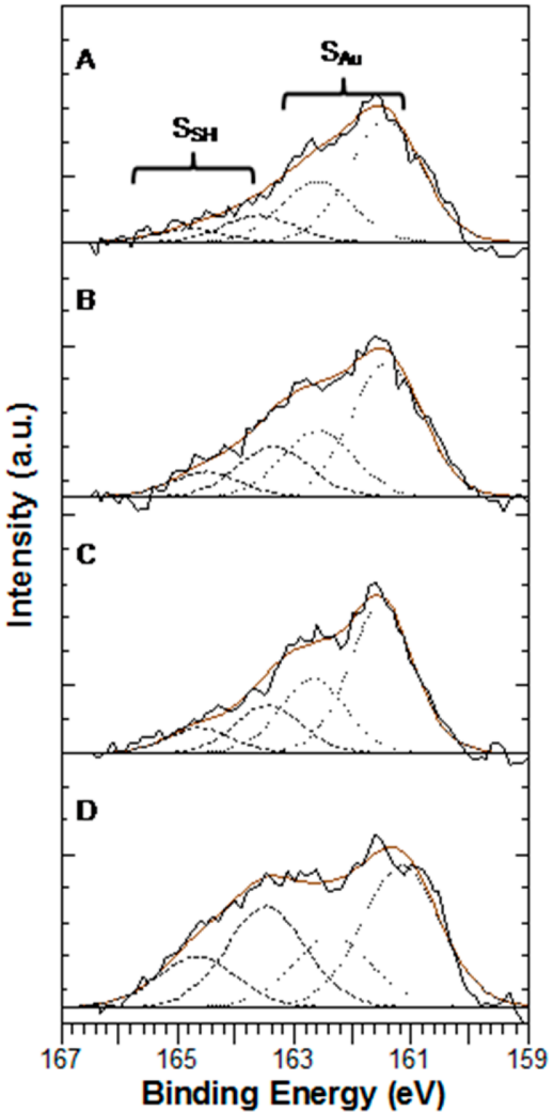

Figure 2. XPS spectra measured at high energy resolution in the S 2p region on gold surfaces modified with aminolyzed P(DMA-*co*-TlaAm)-*x*-SH copolymers of varying composition: *x* = (a) 5, (b) 10, (c) 15, and (d) 30. The continuous line fits the experimental data based on decomposition (dotted lines) of S 2p peak in S $2p_{1/2}$ and S $2p_{3/2}$ singlets for unbound sulfur atoms (free thiol groups, S_{SH}) and sulfur atoms linked to Au (S_{Au}).

Table 3. Percentage of Free Thiol Groups Present in the Copolymer Layers, Determined by XPS

copolymer layer	$S_{SH}/(S_{SH} + S_{Au})$ (%)
P(DMA-*co*-TlaAm)-5-SH	20 ± 3
P(DMA-*co*-TlaAm)-10-SH	30 ± 2
P(DMA-*co*-TlaAm)-15-SH	27 ± 3
P(DMA-*co*-TlaAm)-30-SH	42 ± 2

Grafting of Rhod B-PEG-SH on the Copolymer Layers. P(DMA-*co*-TlaAm)-30-SH layers were selected for the grafting

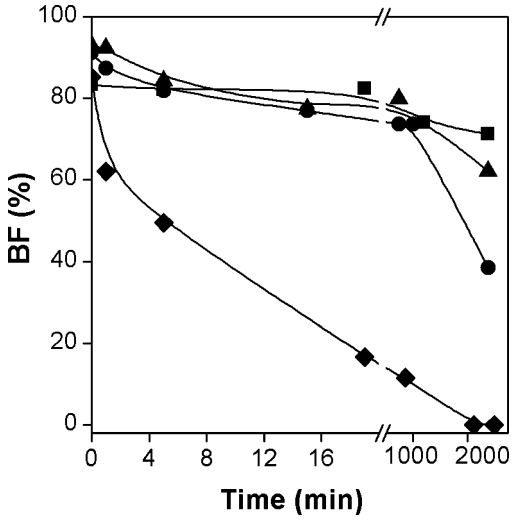

Figure 3. Effect of the oxidizing agent (CaT) on the stability of the P(DMA-*co*-TlaAm)-*x*-SH layers, monitored by cyclic voltammetric measurements: x = 5 (diamond), 10 (circle), 15 (triangle), and 30 (square). The lines are drawn as guide for the eye.

tests due to their higher stability toward oxidizing conditions. The grafting reaction proceeded by immersing a modified gold surface in a CaT/Rhod B-PEG-SH mixture. The Rhod B-PEG-SH reagent was added in excess to enhance the thiol−disulfide exchange toward the formation of disulfide links between thiolated PEG and free thiol groups of the copolymer, and to prevent the formation of intramolecular disulfide bonds between free thiols of the copolymer. The measurement by XRR and XPS of the layer thickness after grafting of Rhod B-PEG-SH did not provide any significant variation compared to the unmodified copolymer layer (Table 2). However, the observation of the modified surface by fluorescence microscopy revealed the presence of the rhodamine-labeled PEG as shown in Figure 4. A similar treatment performed on the surface without CaT did not provide fluorescence (result not shown). Altogether, these results are in agreement with the chemical grafting of the thiolated PEG derivative on the copolymer layer and not on the gold surface. However, the amount of Rhod B-PEG-SH (M_w = 3 400 g mol^{-1}) grafted on the copolymer is too low to induce a measurable variation of the layer thickness.

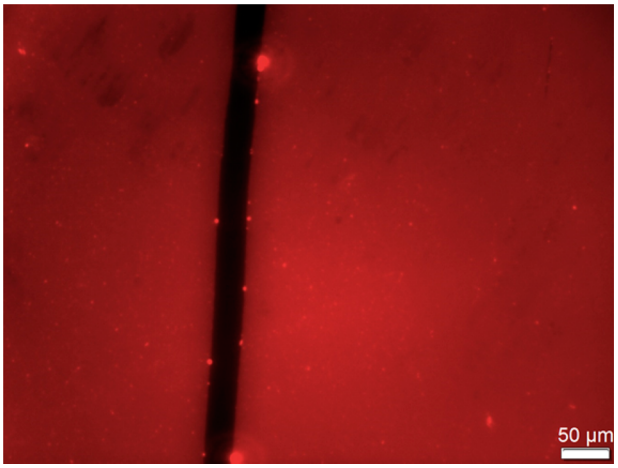

Figure 4. Fluorescence image of a gold surface modified with a P(DMA-*co*-TlaAm)-30-SS-Rhod layer. A deliberate scratch (black line) was made on the surface to show the fluorescence difference between the uncovered background and the grafted layer.

As the modification of a gold surface by resistive layers results in its passivation and hence alters its impedance characteristics, the grafting of the thiolated PEG derivative on a P(DMA-*co*-TlaAm)-30-SH layer was also studied by EIS (Figure 5). The experimental data were fitted to a Randle's equivalent circuit to determine R_{ct} and surface coverage values (Figure 5C). As shown on Nyquist curves displayed in Figures 5A and 5B, the EIS response measured for a bare gold electrode (Figure 5B, curve a) is nearly a straight line, which implies a very low electron transfer resistance (Figure 5C). After modification with the copolymer (Figure 5B, curve b), a higher R_{ct} and surface coverage (determined from eq 2) were observed (Figure 5C), demonstrating the deposition of a polymer layer on the electrode surface. After incubation with Rhod B-PEG-SH in the presence of CaT (Figure 5A, curve c), a further increase of R_{ct} and surface coverage (Figure 5C) was induced due to the grafting of the PEG derivative on the layer.

Release of Grafted Rhod B-PEG-SH in Reducing Conditions. The release of the grafted labeled PEG was tested in the presence of DTT used as a reducing agent to cleave the disulfide bonds formed between the thiol groups of the copolymer and the Rhod B-PEG-SH. It is important to note that CV measurements performed on unmodified P(DMA-*co*-TlaAm)-30-SH layer showed that the presence of DTT in the medium did not affect the stability of the copolymer layer (result not shown). Fluorescence microscopy measurements were first done on a P(DMA-*co*-TlaAm)-30-SS-Rhod layer. A rapid disappearance of the fluorescence of the surface was observed as soon as the sample was placed in a DTT solution, evidencing the successful release of the dye (result not shown).

QCM-D measurements were also performed on a similar grafted layer to estimate the amount of Rhod-PEG-SH released in the medium. For this, a modified quartz substrate was immersed in HEPES buffer and after an equilibrium time of a few minutes, DTT was added in the measuring cell. This addition induced a decrease of the frequency shift due to the change of the medium composition (Figure 6). However, as soon as the quartz surface was rinsed with HEPES buffer, the frequency shift increased to reach a plateau whose value was higher than the initial value measured before addition of DTT. Inversely, the dissipation shift increased with DTT addition and then decreased to a value slightly lower than the initial value upon rinsing. Altogether, these results are in agreement with the loss of deposited matter at the interface after DTT treatment, i.e., to the release of Rhod B-PEG-SH from the surface. The amount of labeled PEG released from the surface was roughly estimated from the Sauerbrey equation (eq 4) to ca. 35 ng cm^{-2}, which corresponds to 0.06 molecule.nm^{-2}. Similar release tests were done on gold nanoparticles modified with a P(DMA-*co*-TlaAm)-30-SS-Rhod layer. The amount of labeled PEG molecules released in the supernatant after DTT addition was measured by fluorescence spectroscopy and was determined to ca. 0.02 molecule nm^{-2}. Although this value is slightly lower than the one measured by QCM-D on flat surfaces, it is of the same order of magnitude. The difference may be attributed to a lower density of copolymer chains immobilized on nanoparticles compared to flat surfaces, as well as to the limits of the Sauerbrey equation in liquid medium.

Interestingly, EIS measurements performed on a modified electrode evidenced that the thiolated PEG derivative could be grafted on a copolymer layer (Figure 5A, curve c), subsequently

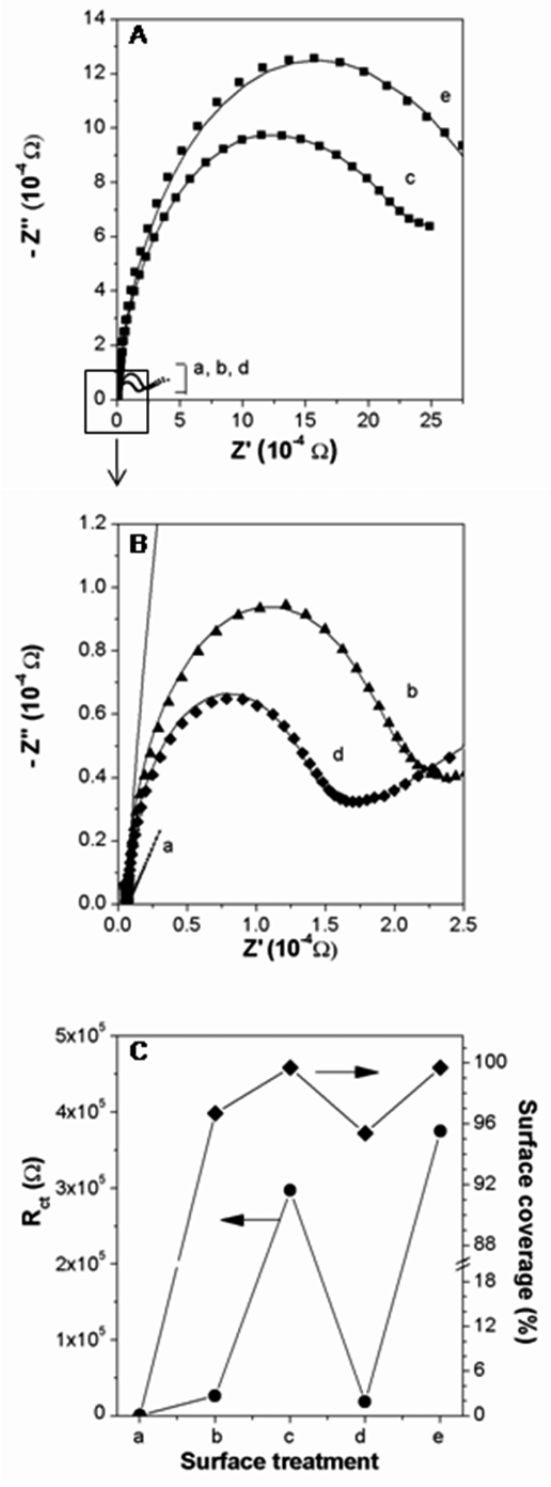

Figure 5. (A) Nyquist plots of electrochemical impedance spectra measured in (a) the presence of $Fe(CN)_6^{3-/4-}$ (1 mM in 0.1 M KCl) for a bare gold electrode, then (b) modified with a P(DMA-*co*-TlaAm)-30-SH layer, (c) subsequently treated with Rhod B-PEG-SH in the presence of CaT, (d) DTT, and (e) again with Rhod B-PEG-SH in the presence of CaT. The continuous lines represent the EIS simulation according to a Randle's equivalent circuit. (B) Zoom-in of graph A; (C) Variation of R_{ct} and surface coverage determined from the EIS simulations performed on experimental data measured after the different surface treatments (from a to e).

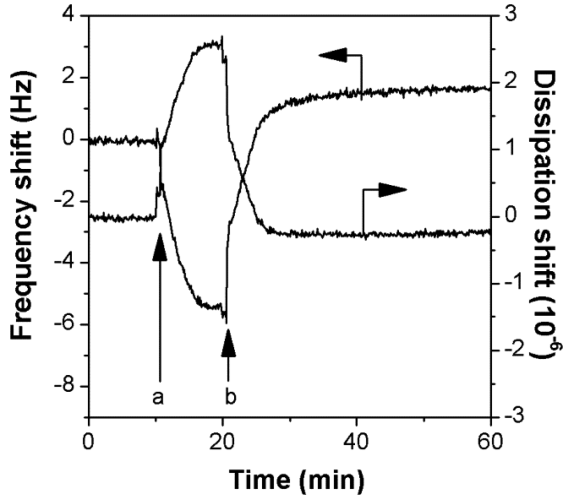

Figure 6. QCM-D measurements performed on a gold-coated sensor, modified ex situ with a P(DMA-*co*-TlaAm)-30-SS-Rhod layer and subsequently treated in situ with DTT. The sample was initially placed in contact with HEPES buffer; after an equilibrium time of 10 min, HEPES buffer was (a) replaced by a 0.1 M DTT solution for 10 min, then (b) rinsed with HEPES buffer. The normalized frequency shift and dissipation shift are shown for the third overtone.

released by adding DTT in the medium (Figure 5B, curve d) and regrafted by a further incubation in the presence of CaT (Figure 5A, curve e). The reversible grafting/release of the thiolated PEG through the formation and cleavage of the disulfide link under redox stimulation, induced reproducible up and down variations of R_{ct} and surface coverage, as shown in Figure 5C. These results demonstrate the rapid and reversible redox-responsive behavior of our system.

CONCLUSION

We showed here that copolymers containing thiolactone units can be used as stable precursors to produce, in one step, stable polythiol layers grafted onto gold surfaces. Ring-opening of the thiolactones in the presence of an amine derivative results in the formation of thiol groups along the macromolecular chains. These thiol groups can be used for both immobilization on a gold surface and postgrafting of a thiolated derivative of interest. We demonstrated that the fraction of free thiols available in the immobilized copolymer layer for the subsequent grafting can be tuned as a function of the initial composition of the copolymer. However, only the copolymers with a high content of thiolactone units are stable under redox stimulation. These layers were successfully functionalized with a thiolated dye, used as a model drug, to illustrate the reversible grafting process. It was shown that the dye can be released in reducing conditions and again regrafted in oxidizing conditions. These grafting/release cycles can be performed in a reproducible way, which testifies for the stimuli-responsive behavior of the system.

Our strategy based on thiolactone-containing copolymers for the one-step preparation of polythiol layers, combined with the subsequent grafting of a thiolated substance of interest, through a cleavable disulfide bond, provides an easy way to produce redox-responsive layers with controlled release properties. Applied on more sophisticated surfaces such as surfaces with topographic patterns, these functionalized redox-responsive layers will allow the functionality of the surface to be controlled spatially and temporally, to further direct cell behavior.

dx.doi.org/10.1021/am506489j | ACS Appl. Mater. Interfaces 2014, 6, 22457−22466

■ ASSOCIATED CONTENT

Supporting Information

Chemical composition (measured by XPS), XRR results, and contact angles of gold surfaces modified with aminolyzed P(DMA-*co*-TlamAm)-*x*-SH layers. This material is available free of charge via the Internet at http://pubs.acs.org.

■ AUTHOR INFORMATION

Corresponding Authors

*E-mail: karine.glinel@uclouvain.be. Phone: ++ 32 10 47 35 58. Fax: ++ 32 10 45 15 93;
*E-mail: sophie.demoustier@uclouvain.be. Phone: ++ 32 10 47 27 02. Fax: ++ 32 10 45 15 93.

Author Contributions

The manuscript was written through contributions of all authors. All authors have given approval to the final version of the manuscript.

Notes

The authors declare no competing financial interest.

■ ACKNOWLEDGMENTS

This research was supported by Belgian Federal Science Policy (IAP program P7/05). Tom Plankaert is acknowledged for the performed elemental analysis. Dr. A. Fernandes and Dr. I. Kacem are thanked for their technical assistance with XRR and electrochemical measurements, respectively. S.R., P.E., and F.D.P. are thankful to Ghent University for financial support. K.G. is a Research Associate of the F.R.S.-FNRS.

■ REFERENCES

(1) Sinn Aw, M.; Kurian, M.; Losic, D. Non-Eroding Drug-Releasing Implants with Ordered Nanoporous and Nanotubular Structures: Concepts for Controlling Drug Release. *Biomater. Sci.* **2014**, *2*, 10−34.
(2) Chung, H. J.; Park, T. G. Surface Engineered and Drug Releasing Pre-Fabricated Scaffolds for Tissue Engineering. *Adv. Drug Delivery Rev.* **2007**, *59*, 249−262.
(3) Goldberg, M.; Langer, R.; Jia, X. Nanostructured Materials for Applications in Drug Delivery and Tissue Engineering. *J. Biomater. Sci., Polym. Ed.* **2007**, *18*, 241−268.
(4) Stuart, M. A. C.; Huck, W. T. S.; Genzer, J.; Müller, M.; Ober, C.; Stamm, M.; Sukhorukov, G. B.; Szleifer, I.; Tsukruk, V. V.; Urban, M.; Winnik, F.; Zauscher, S.; Luzinov, I.; Minko, S. Emerging Applications of Stimuli-Responsive Polymer Materials. *Nat. Mater.* **2010**, *9*, 101−113.
(5) Roy, D.; Cambre, J. N.; Sumerlin, B. S. Future Perspectives and Recent Advances in Stimuli-Responsive Materials. *Prog. Polym. Sci.* **2010**, *35*, 278−301.
(6) Bawa, P.; Pillay, V.; Choonara, Y. E.; Du Toit, L. C. Stimuli-Responsive Polymers and their Applications in Drug Delivery. *Biomed. Mater.* **2009**, *4*, 022001.
(7) Sershen, S.; West, J. Implantable, Polymeric Systems for Modulated Drug Delivery. *Adv. Drug Delivery Rev.* **2002**, *54*, 1225−1235.
(8) de la Rica, R.; Aili, D.; Stevens, M. M. Enzyme-Responsive Nanoparticles for Drug Release and Diagnostics. *Adv. Drug Delivery Rev.* **2012**, *64*, 967−978.
(9) Traitel, T.; Goldbart, R.; Kost, J. Smart Polymers for Responsive Drug-Delivery Systems. *J. Biomater. Sci., Polym. Ed.* **2008**, *19*, 755−767.
(10) Huo, M.; Yuan, J.; Tao, L.; Wei, Y. Redox-Responsive Polymers for Drug Delivery: From Molecular Design to Applications. *Polym. Chem.* **2014**, *5*, 1519−1528.
(11) Meng, F.; Hennink, W. E.; Zhong, Z. Reduction-Sensitive Polymers and Bioconjugates for Biomedical Applications. *Biomaterials* **2009**, *30*, 2180−2198.
(12) Li, C.; Zhao, S.; Li, J.; Yin, Y. Polymeric Biomaterials Containing Thiol/Disulfide Bonds. *Prog. Chem.* **2013**, *25*, 122−134.
(13) Saito, G.; Swanson, J. A.; Lee, K. D. Drug Delivery Strategy Utilizing Conjugation via Reversible Disulfide Linkages: Role and Site of Cellular Reducing Activities. *Adv. Drug Delivery Rev.* **2003**, *55*, 199−215.
(14) Akita, H.; Ishiba, R.; Hatakeyama, H.; Tanaka, H.; Sato, H.; Tange, K.; Arai, M.; Kubo, K.; Harashima, H. A Neutral Envelope-Type Nanoparticle Containing pH-Responsive and SS-Cleavable Lipid-like Material as a Carrier for Plasmid DNA. *Adv. Healthcare Mater.* **2013**, *2*, 1120−1125.
(15) Brülisauera, L.; Gauthier, M. A.; Leroux, J. C. Disulfide-Containing Parenteral Delivery Systems and their Redox-Biological Fate. *J. Controlled Release* **2014**, DOI: 10.1016/j.jconrel.2014.06.012.
(16) Zelikin, A. N.; Quinn, J. F.; Caruso, F. Disulfide Cross-Linked Polymer Capsules: En Route to Biodeconstructible Systems. *Biomacromolecules* **2005**, *7*, 27−30.
(17) Shimoni, O.; Postma, A.; Yan, Y.; Scott, A. M.; Heath, J. K.; Nice, E. C.; Zelikin, A. N.; Caruso, F. Macromolecule Functionalization of Disulfide-bonded Polymer Hydrogel Capsules and Cancer Cell Targeting. *ACS Nano* **2012**, *6*, 1463−1472.
(18) Tang, L. Y.; Wang, Y. C.; Li, Y.; Du, J. Z.; Wang, J. Shell-Detachable Micelles based on Disulfide-linked Block Copolymer as Potential Carrier for Intracellular Drug Delivery. *Bioconjugate Chem.* **2009**, *20*, 1095−1099.
(19) Yan, Y.; Wang, Y.; Heath, J. K.; Nice, E. C.; Caruso, F. Cellular Association and Cargo Release of Redox-Responsive Polymer Capsules Mediated by Exofacialthiols. *Adv. Mater.* **2011**, *23*, 3916−3921.
(20) Lee, S. Y.; Tyler, J. Y.; Kim, S.; Park, K.; Cheng, J. X. FRET Imaging Reveals Different Cellular entry Routes of Self-Assembled and Disulfide Bonded Polymeric Micelles. *Mol. Pharmaceutics* **2013**, *10*, 3497−3506.
(21) López-Mirabal, H. R.; Winther, J. R. Redox Characteristics of the Eukaryotic Cytosol. *Biochim. Biophys. Acta. Mol. Cell Res.* **2008**, *1783*, 629−640.
(22) Bauhuber, S.; Hozsa, C.; Breunig, M.; Göpferich, A. Delivery of Nucleic Acids via Disulfide-based Carrier Systems. *Adv. Mater.* **2009**, *21*, 3286−3306.
(23) Le Neindre, M.; Nicolaÿ, R. Polythiol Copolymers with Precise Architectures: A Platform for Functional Materials. *Polym. Chem.* **2014**, *5*, 4601−4611.
(24) West, K. R.; Otto, S. Reversible Covalent Chemistry in Drug Delivery. *Curr. Drug Discovery Technol.* **2005**, *2*, 123−160.
(25) Capozzi, G.; Modena, G. Oxidation of thiols. In *The Thiol Group*; Patai, S., Ed.; John Wiley & Sons: Chichester, U.K., 1974; Vol. 2, pp 785−839.
(26) Espeel, P.; Du Prez, F. E. One-Pot Multi-Step reactions based on Thiolactone Chemistry: A Powerful Synthetic Tool in Polymer Science. *Eur. Polym. J.* **2014**, DOI: 10.1016/j.eurpolymj.2014.07.008.
(27) Espeel, P.; Goethals, F.; Du Prez, F. E. One-Pot Multistep Reactions based on Thiolactones: Extending the Realm of Thiol-ene Chemistry in Polymer Synthesis. *J. Am. Chem. Soc.* **2011**, *133*, 1678−1681.
(28) Espeel, P.; Goethals, F.; Driessen, F.; Nguyen, L.T. T.; Du Prez, F. E. One-Pot, Additive-Free Preparation of Functionalized Polyurethanes via Amine-Thiol-Ene Conjugation. *Polym. Chem.* **2013**, *4*, 2449−2456.
(29) Goethals, F.; Martens, S.; Espeel, P.; Van Den Berg, O.; Du Prez, F. E. Diversely Substituted Polyamide sSructures through Thiol-Ene Polymerization of Renewable Thiolactone Building Blocks. *Macromolecules* **2014**, *47*, 61−69.
(30) Espeel, P.; Goethals, F.; Stamenović, M. M.; Petton, L.; Du Prez, F. E. Double Modular Modification of Thiolactone-Containing Polymers: Towards Polythiols and Derived Structures. *Polym. Chem.* **2012**, *3*, 1007−1015.
(31) Reinicke, S.; Espeel, P.; Stamenović, M. M.; Du Prez, F. E. One-Pot Double Modification of p(NIPAAm): A Tool for Designing

Tailor-Made Multiresponsive Polymers. *ACS Macro Lett.* **2013**, *2*, 539−543.
(32) Stamenović, M. M.; Espeel, P.; Baba, E.; Yamamoto, T.; Tezuka, Y.; Du Prez, F. E. Straightforward Synthesis of Functionalized Cyclic Polymers in High Yield via RAFT and Thiolactone-Disulfide Chemistry. *Polym. Chem.* **2013**, *4*, 184−193.
(33) Chen, Y.; Espeel, P.; Reinicke, S.; Du Prez, F. E.; Stenzel, M. H. Control of Glycopolymer Nanoparticle Morphology by a One-Pot, Double Modification Procedure using Thiolactones. *Macromol. Rapid Commun.* **2014**, *35*, 1128−1134.
(34) Reinicke, S.; Espeel, P.; Stamenović, M. M.; Du Prez, F. E. Synthesis of Multi-Functionalized Hydrogels by a Thiolactone-based Synthetic Protocol. *Polym. Chem.* **2014**, *5*, 5461−5470.
(35) Espeel, P.; Carrette, L. L. G.; Bury, K.; Capenberghs, S.; Martins, J. C.; Duprez, F. E. Madder, A. Multifunctionalized Sequence-Defined Oligomers from a Single Building Block. *Angew. Chem., Int. Ed.* **2013**, *52*, 13261−13264.
(36) K'Owino, I. O.; Sadik, O. A. Impedance Spectroscopy: a Powerful Tool for Rapid Biomolecular Screening and Cell Culture Monitoring. *Electroanalysis* **2005**, *17*, 2101−2113.
(37) Ribaut, C.; Reybier, K.; Torbiero, B.; Launay, J.; Valentin, A.; Reynes, O.; Fabre, P. L.; Nepveu, F. Strategy of Red Blood Cells Immobilisation onto a Gold Electrode: Characterization by Electrochemical Impedance Spectroscopy and Quartz Crystal Microbalance. *IRBM* **2008**, *29*, 141−148.
(38) Sahoo, R. R.; Patnaik, A. Binding of Fullerene C60 to Gold Surface Functionalized by Self-Assembled Monolayers of 8-Amino-1-Octane Thiol: A Structure Elucidation. *J. Colloid Interface Sci.* **2003**, *268*, 43−49.
(39) Genet, M. J.; Dupont-Gillain, C. C.; Rouxhet, P. G. XPS Analysis of Biosystems and Biomaterials. In *Medical Applications of Colloids*; Matijevic, E., Ed.; Springer Science: New York, 2008; pp 177−307.
(40) Tanuma, S.; Powell, C. J.; Penn, D. R. Calculations of Electron Inelastic Mean Free Paths. II. Data for 27 Elements over the 50−2000 eV Range. *Surf. Interface Anal.* **1991**, *17*, 911−926.
(41) Powell, C. J.; Jablonski, A. *Electron Inelastic Mean Free Path Database, Version 1.1 (SRD71)*; U.S. Department of Commerce, National Institute of Standards and Technology: Gaithersburg, MD, 2000.
(42) Sauerbrey, G. Use of Quartz Vibrator for Weighing Thin Layers and as a Micro-Balance. *Z. Physik* **1959**, *155*, 206−222.
(43) Arys, X.; Laschewsky, A.; Jonas, A. M. Ordered Polyelectrolyte ″Multilayers″ - 1. Mechanisms of Growth and Structure Formation: A Comparison with Classical Fuzzy "Multilayers". *Macromolecules* **2001**, *34*, 3318−3330.
(44) Cecchet, F.; Marcaccio, M.; Margotti, M.; Paolucci, F.; Rapino, S.; Rudolf, P. Redox Mediation at 11-Mercaptoundecanoic Acid Self-Assembled Monolayers on Gold. *J. Phys. Chem. B* **2006**, *110*, 2241−2248.
(45) Lowe, A. B;; Bowman. C. N. *Thiol-X Chemistries in Polymer and Materials Science*; Royal Society of Chemistry: Cambridge, U.K., 2013.
(46) Lebec, V.; Landoulsi, J.; Boujday, S.; Poleunis, C.; Pradier, C. M.; Delcorte, A. Probing the Orientation of *β*-Lactoglobulin on Gold Surfaces Modified by Alkyl Thiol Self-Assembled Monolayers. *J. Phys. Chem. C* **2013**, *117*, 11569−11577.
(47) Shon, Y. S.; Kelly, K. F.; Halas, N. J.; Lee, T. R. Fullerene-Terminated Alkanethiolate SAMs on Gold Generated from Unsymmetrical Disulfides. *Langmuir* **1999**, *15*, 5329−5332.
(48) Sun, F.; Grainger, D. W.; Castner, D. G.; Leach-Scampavia, D. K. Adsorption of Ultrathin Films of Sulfur-Containing Siloxane Oligomers on Gold Surfaces and their in situ Modification. *Macromolecules* **1994**, *27*, 3053−3062.
(49) Bain, C. D.; Troughton, E. B.; Tao, Y. T.; Evall, J.; Whitesides, G. M.; Nuzzo, R. G. Formation of Monolayer Films by the Spontaneous Assembly of Organic Thiols from Solution onto Gold. *J. Am. Chem. Soc.* **1989**, *111*, 321−335.
(50) Davies, M. J.; Hawkins, C. L. Hypochlorite-Induced Oxidation of Thiols: Formation of Thiyl Radicals and the Role of Sulfenyl Chlorides as Intermediates. *Free Radical Res.* **2000**, *33*, 719−729.
(51) Finley, J. W.; Wheeler, E. L.; Witt, S. C. Oxidation of Glutathione by Hydrogen Peroxide and other Oxidizing Agents. *J. Agric. Food Chem.* **1981**, *29*, 404−407.
(52) Li, Y.; Armes, S. P. Synthesis and Chemical Degradation of Branched Vinyl Polymers Prepared via ATRP: Use of a Cleavable Disulfide-based Branching Agent. *Macromolecules* **2005**, *38*, 8155−8162.